

3-1-2011

Chemical response of lithiated graphite with deuterium irradiation

C. N. Taylor

Birck Nanotechnology Center, Purdue University, ctaylor@purdue.edu

B. Heim

Birck Nanotechnology Center, Purdue University

Jean Paul Allain

Birck Nanotechnology Center, Purdue University, allain@purdue.edu

Follow this and additional works at: <http://docs.lib.purdue.edu/nanopub>



Part of the [Nanoscience and Nanotechnology Commons](#)

Taylor, C. N.; Heim, B.; and Allain, Jean Paul, "Chemical response of lithiated graphite with deuterium irradiation" (2011). *Birck and NCN Publications*. Paper 1039.

<http://dx.doi.org/10.1063/1.3555097>

This document has been made available through Purdue e-Pubs, a service of the Purdue University Libraries. Please contact epubs@purdue.edu for additional information.

Chemical response of lithiated graphite with deuterium irradiation

C. N. Taylor, B. Heim, and J. P. Allain

Citation: *J. Appl. Phys.* **109**, 053306 (2011); doi: 10.1063/1.3555097

View online: <http://dx.doi.org/10.1063/1.3555097>

View Table of Contents: <http://jap.aip.org/resource/1/JAPIAU/v109/i5>

Published by the AIP Publishing LLC.

Additional information on J. Appl. Phys.

Journal Homepage: <http://jap.aip.org/>

Journal Information: http://jap.aip.org/about/about_the_journal

Top downloads: http://jap.aip.org/features/most_downloaded

Information for Authors: <http://jap.aip.org/authors>

ADVERTISEMENT

The advertisement banner for AIP Advances features a light green background with a pattern of thin, curved, wavy lines in a darker green shade. The AIP Advances logo is centered, with 'AIP' in blue and 'Advances' in green, accompanied by a series of orange dots of varying sizes. To the right, a circular seal states 'Now Indexed in Thomson Reuters Databases'. Below the logo, the text 'Explore AIP's open access journal:' is followed by a list of three bullet points: 'Rapid publication', 'Article-level metrics', and 'Post-publication rating and commenting'.

AIPAdvances

Now Indexed in
Thomson Reuters
Databases

Explore AIP's open access journal:

- Rapid publication
- Article-level metrics
- Post-publication rating and commenting

Chemical response of lithiated graphite with deuterium irradiation

C. N. Taylor,^{1,2,a)} B. Heim,^{1,2} and J. P. Allain^{1,2}¹Purdue University, School of Nuclear Engineering, West Lafayette, Indiana 47907, USA²Birck Nanotechnology Center, Discovery Park, West Lafayette, Indiana 47907, USA

(Received 20 October 2010; accepted 14 January 2011; published online 15 March 2011)

Lithium wall conditioning has been found to enhance plasma performance for graphite walled fusion devices such as TFTR, CDX-U, T-11M, TJ-II and NSTX. Among observed plasma enhancements is a reduction in edge density and reduced deuterium recycling. The mechanism by which lithiated graphite retains deuterium is largely unknown. Under controlled laboratory conditions, X-ray photoelectron spectroscopy (XPS) is used to observe the chemical changes that occur on ATJ graphite after lithium deposition. The chemical state of lithiated graphite is found to change upon deuterium irradiation indicating the formation Li-O-D, manifest at 532.9 ± 0.6 eV. Lithium-deuterium interactions are also manifest in the C 1s photoelectron energy range and show Li-C-D interactions at 291.2 ± 0.6 eV. Post-mortem NSTX tiles that have been exposed to air upon extraction are cleaned and examined, revealing the chemical archaeology that formed during NSTX operations. XPS spectra show strong correlation (± 0.3 eV) in Li-O-D and Li-O peaks from post-mortem and control experiments, thus validating offline experiments. We report findings that show that deuterium is found to interact with lithium after lithium has already reacted with carbon and oxygen. © 2011 American Institute of Physics. [doi:10.1063/1.3555097]

I. INTRODUCTION

Lithium as a plasma-facing surface has been investigated in various fusion devices including TFTR, CDX-U, FTU, T-11M and NSTX, as a means of enhancing plasma performance. Specifically for NSTX, improvements include a reduction of edge localized modes (ELMs) in H-mode plasmas¹, and reduced recycling.^{2–4} Recycling occurs when wall deuterium re-enters the plasma via reflection, desorption, and hydrocarbon emission, among other possible channels. Lithium coatings on graphite plasma facing components (PFC) enhance deuterium retention and reduce recycling. Lithium wall conditioning in NSTX has employed the use of lithium pellet injection (LPI), addition of a lithium evaporator (LiTER) to increase deposition rate, and two LiTERs⁵ for greater vessel coverage and deposition. Each successive lithium deposition method has resulted in increased improvements in particle control and recycling. A liquid lithium divertor (LLD) is the next step in NSTX lithium PFC research and is expected to provide a “self healing” plasma facing surface.^{3,6}

Plasma-surface interactions are found to drastically affect plasma performance within fusion devices. Therefore, understanding fundamental plasma surface interactions is essential to the development of plasma facing components that will not hinder a sustained fusion reaction. Presently, surface chemistry techniques, namely X-ray photoelectron spectroscopy (XPS), are used to interrogate graphite surfaces before and after various surface modifications that occur in lithium conditioned fusion devices.

Lithium is of interest throughout various disciplines due to its use in lithium batteries⁷ and hydrogen storage,⁸ among other varied uses.⁹ Consequently lithium surfaces have been

examined extensively, including pertinent studies of lithium-graphite intercalation.^{10,11} Additionally, investigations regarding the chemical state of lithiated graphite have been conducted and show that lithated graphite readily forms lithium carbonate when exposed to air.¹² In more fusion relevant studies lithium-deuterium interactions were examined and results indicate that liquid lithium binds with energetic deuterium in the form of LiD.¹³ The mechanism by which lithiated graphite retains deuterium remains largely unknown. Here, we study the chemical interactions that occur when lithium is deposited on ATJ graphite, and more notably, we examine the surface chemistry resultant of deuterium irradiation. Results from our offline experiments are compared to XPS analysis of NSTX post-mortem tiles.

II. EXPERIMENTAL SETUP

Samples are made from 12.7 mm diameter, high-temperature conductive, fine grain (.03 mm) ATJ graphite (Graf-Tech, formerly Union Carbide – a provider for NSTX tiles).³ Samples are cut into 2–3 mm thicknesses. Sample surface is polished to reduce morphology effects that can arise in surface characterization. Morphology effects can include an effective thinning of nominal lithium thickness and photoelectron shadowing. All experimental work including sample preparation, surface modification, and analysis is performed in an Omicron surface analysis suite, located in the Birck Nanotechnology Center at Purdue University.

The Omicron surface analysis facility employs a variety of methods to analyze the surface chemistry and physical properties of sample substrates. Characterization capabilities include techniques such as quadrupole mass spectrometry (QMS), thermal desorption spectroscopy (TDS), X-ray photoelectron spectroscopy (XPS), high-resolution electron energy-loss spectroscopy (HR-EELS), and contains *in situ*

^{a)}Electronic mail: ctaylor@purdue.edu.

scanning electron microscopy (SEM). An Omicron EA 125 hemispherical energy analyzer is used for photoelectron spectroscopy. In addition, the facility employs several methods for surface modification including evaporation sources, ion guns, and x-ray sources.

Lithium is deposited using a custom-built lithium evaporation and deposition system (LEDS). LEDS heats and evaporates lithium in a crucible-filament configuration. Lithium is loaded under argon atmosphere into the crucible to avoid oxidation. A nose cone is attached to LEDS to contain the lithium evaporant and collimate the efflux to a ~ 1 cm diameter spot size. Deposition rate is monitored and calibrated using a quartz crystal microbalance (QCM), prior to each evaporation, in order to deposit a desired nominal dose. Disparity between the desired nominal dose and the actual thickness results from sample roughness. Microsurface features increase sample surface area. For a given lithium dose, the increase in surface area would result in a lithium layer that is thinner than the desired nominal thickness. In addition, rapid lithium intercalation into graphite causes the nominal lithium dose to be effectively thinned with time. QCM measurements for monitoring nominal deposition thickness have been cross calibrated via cross sectional scanning electron microscopy (XSEM), resulting in a 6.5% error when depositing a 2 μm film on silicon.

Current NSTX lithium conditioning is typically applied between discharges for periods between 5–15 min at ~ 20 –80 mg/min.² Assuming that lithium coating reaches 25% of NSTX's 40 m² interior surface area, a nominal lithium thickness of ~ 38 –151 nm would result from a typical 10 min deposition. Over the course of a campaign, over 100 g of lithium is deposited, resulting in a deposition layer >20 μm . For Purdue controlled experiments, the goal is to replicate mid-cycle lithium conditions. For this reason, a nominal lithium thickness of 2.0 ± 0.13 μm (at a maximum deposition rate of ~ 25 Å/s) is typically used in offline experiments. A lithium layer thicker or thinner than 2 μm is found to affect the capacity of deuterium retention and is not the topic of this work, but is discussed elsewhere.¹⁴

Lithiated graphite samples are exposed to a deuterium ion flux of $\Gamma \approx 7 \times 10^{13}$ cm⁻²s⁻¹ at 500 eV/amu (1 keV for D_2^+) using an Omicron ISE-10 ion gun. NSTX ion temperature measurements are typically <1.1 keV.² Samples are irradiated at room temperature (22 °C) for periods ranging from 1 min (4.2×10^{13} cm⁻²) to 5 hs (1.3×10^{18} cm⁻²). NSTX deuterium flux varies greatly depending on the measurement location but in the lower divertor the particle flux is on the order of 10^{18} s⁻¹cm⁻² (10^{22} s⁻¹m⁻²).¹⁵ Ion angle of incidence ranges from surface normal to 30° from normal and no changes in surface chemistry are observed with varying angle. NSTX field lines vary throughout the torus and divertor locations can have field angles of a few degrees.¹⁶

ATJ graphite substrates are characterized and analyzed in their virgin state and after each surface modification (i.e., post lithiumization and deuterium irradiation) using X-ray photoelectron spectroscopy (XPS). Via the photoelectric effect, incident x-rays eject inner core photoelectrons from the sample surface which are then collected by an energy selective hemispherical analyzer. Because elements and

chemical bonds have characteristic photoelectron binding energies, XPS provides a valuable tool in qualitative analysis for determining binding functionalities. The probing depth of XPS is ~ 10 nm and thus is within range of the implanted deuterium ions. A nonmonochromatic Al K α source (1486.6 eV) is used for the X-ray production. Analyzer resolution (0.6 eV) and statistical standard error (SE) contribute to XPS spectral error. The XPS spectra in this study have a SE of less-than 0.02 eV and therefore error propagation is dominated by analyzer resolution.

NSTX divertor tiles were removed from varying radial and toroidal locations from within the vessel and were cored into ~ 1 -cm diameter disks. NSTX post-mortem tiles are exposed to air upon removal from NSTX and form a surface passivation layer. Fortuitously, the passivation layer is found to act as barrier that protects the archaeology of lithium interactions that formed during plasma operations. In order to uncover this history, a cleaning procedure of sputtering and occasionally annealing is used. Sputter cleaning utilizes 1 keV Ar for ~ 30 mins ($\Gamma \approx 10^{13}$ cm⁻²s⁻¹). For samples extracted from the lower divertor private flux region (PFR), it is found that sputtering cleaning alone will not fully remove the passivated layer, which is manifest as a broad disordered peak in the photoelectron spectrum, indicating a possible amorphous structure (shown later in Fig. 6). Graphite surfaces exposed to the high-density, low-temperature deuterium plasma of the PFR typically transform into an amorphous phase with high deuterium content and dangling bonds on the surface that ultimately uptake large quantities of oxygen and nitrogen when exposed to air.

Annealing of these samples repairs the sample surface and restores the photoelectron spectrum to one with characteristic standard spectral lines (e.g., C 1s). The cleaning procedure for passivated tiles is therefore prescribed as sputtering followed by annealing. Samples removed from the PFR, and cleaned after this procedure, unveil two peaks characteristic of Li-O-D interactions, as will be shown hereafter. It will also be shown that the trends seen in offline control samples are consistent with post-cleaned PFR tile samples.

III. RESULTS AND DISCUSSION

A. Lithium and deuterium effects on oxygen chemistry

Virgin ATJ graphite has primary peaks in the photoelectron spectrum at 532.0 ± 0.6 eV and 283.6 ± 0.6 eV, corresponding to O 1s and C 1s respectively. The O 1s peak is Gaussian in appearance, an indication that the spectrum consists of one primary bond (a thorough analysis of the C 1s peaks is presented in the subsequent section). A typical XPS spectrum for virgin ATJ graphite is shown in Fig. 1(a). As-received NSTX post-mortem samples show oxygen bonds that dominate the carbon bonds in the XPS spectrum, characteristic of surface oxidation [Fig. 1(b)]. In addition, lithium is observed at 56 eV.¹⁷

After depositing 2 μm lithium on virgin graphite a second peak develops in the O 1s spectrum at 529.5 ± 0.6 eV as seen in Fig. 3. In the present study, this peak as well as all others, will be referred to by the known chemical

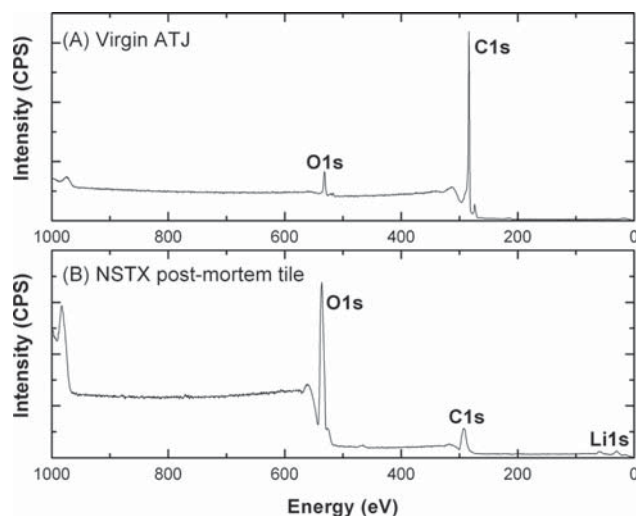


FIG. 1. XPS wide energy range scan showing the prominent photoelectron peaks for (a) virgin ATJ graphite sample, and (b) NSTX post-mortem tile. Primary peaks correspond to the O 1s and C 1s energies.

constituents (i.e., Li-O) as opposed to stoichiometric notation. Thus Li-O refers to a chemical functional group as opposed to a known chemical bond that occurs when lithium is deposited on graphite and is observed in the O 1s spectrum. However, Harilal *et al.* address the development of this peak and attribute it to Li_2O_2 and also find that varying the lithium dose does not affect the location of the peak, but influences the peak intensity relative to the neighboring O peak.¹² In addition to the formation of a Li-O interaction, the C-O peak (formerly located at ~ 532 eV) shifts 0.5 eV to lower binding energy (~ 531.5 eV). The cause of this shift remains the subject of additional studies. Successive XPS spectra of the O 1s energy range immediately following lithium deposition show indications of a highly dynamic system. This behavior is observed in Fig. 2 as the Li-O peak intensity decreases relative to O as time progresses. Over a >37 min period, the presence of Li-O diminishes, an indication of lithium intercalation into the graphite.¹⁰ In addition, over the same temporal scale the binding energy for O-C shifts from its prompt lithium deposition location (531.6 eV) back to ~ 532 eV. This is an indication that lithium may interact by more than one mechanism and form weak bonds that disassociate with time in addition to stronger bonds that remain intact for long periods of time (i.e., Li_2O_2). A ratio of Li-O and O-C integrated peaks is shown in Fig. 3(a). An outlying data point is found at 483 sec and will be investigated further in future studies. Because the $1\ \mu\text{m}$ lithium dose exceeds the probing depth for XPS (<10 nm), the ratio trend appears to be constant for the first ~ 1250 sec. At times >1250 sec, it is apparent that Li-O interactions decrease relative to O-C bonds, thus causing the ratio to decrease. Comparing the maximum and minimum ratios indicates that over 2415 sec, the Li-O/O-C peak ratio varies 14%. Additional experiments have shown that this trend continues for days. For larger lithium doses (i.e., $5\ \mu\text{m}$), this trend is less prominent, and in contrast the slope of the Li-O/O-C ratio is positive instead of negative as in the $1\ \mu\text{m}$ case (Fig. 3b). The ratio increases as

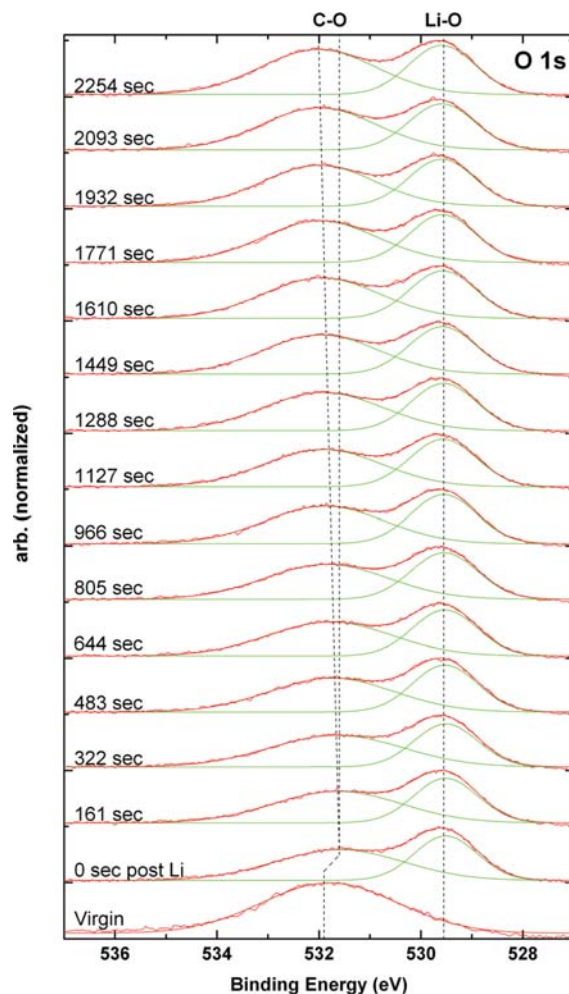


FIG. 2. (Color online) Fifteen consecutive and continuous XPS scans taken (with sample remaining in the analysis chamber at $\sim 1 \times 10^{-9}$ Torr) immediately after lithium deposition show changes in relative peak intensity as well as binding energy for O-C.

a result of either a decrease in surface O-C or an increase in surface Li-O. Following lithium deposition no mechanism is present that would decrease surface O-C, therefore an increase in surface Li-O must stimulate the increasing Li-O/O-C ratio. Lithium is known to form strong bonds with oxygen and act as an oxygen getter.¹⁸ The increase in Li-O on this time scale is an indication that available lithium is getting oxygen.

After lithium conditioning, the samples are irradiated with deuterium at a flux of $7 \times 10^{13}\ \text{cm}^{-2}\text{s}^{-1}$ for 30 mins, achieving a fluence of $9 \times 10^{16}\ \text{cm}^{-2}$. The Li-O peak shifts 0.5 eV to 530.0 ± 0.6 eV, but the CO peak formerly located at 532 eV is replaced with a new peak located at 532.9 ± 0.6 eV, as seen in Fig. 4(a) (labeled 'D2: 30m'). Figure 4(d) shows a separate study in which ATJ graphite was irradiated with a comparable fluence of $\sim 6 \times 10^{16}\ \text{cm}^{-2}$, but with no prior lithium conditioning. In this case deuterium irradiation did not result in the formation of a peak at 532.9 eV. Because this peak is observed only after irradiating *lithiated* graphite, the peak can be attributed to a Li-O-D interaction. Consecutive and continuous spectra taken after deuterium irradiation reveal a system that

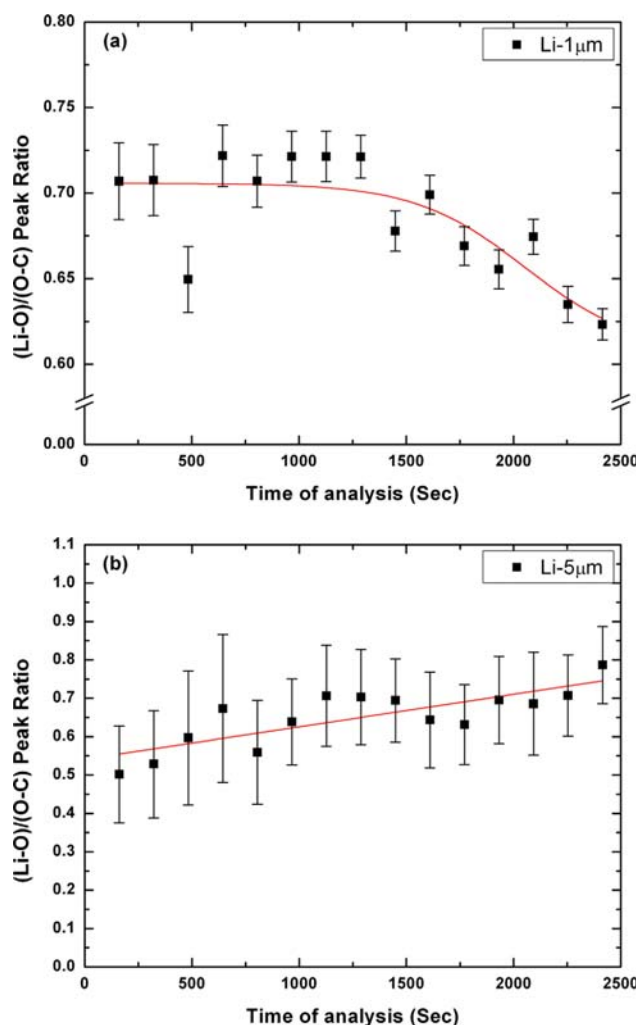


FIG. 3. (Color online) Ratio of integrated peak areas Li-O and O-C (computed as Li-O/O-C) for (a) a $1\text{ }\mu\text{m}$ dose of lithium, and (b) a $5\text{ }\mu\text{m}$ dose of lithium. Curve fits are to guide the eye and in (a) represent a dose-response decay, and in (b) a linear fit was used. Decreasing trend is an indication of intercalation and that Li-O is decreasing relative to O-C, whereas an increasing trend indicates oxygen gettering.

is much more stable than lithiated graphite. Over a period of $>37\text{ min}$, the O-C binding energy shifted only 0.17 eV , whereas after lithium deposition it shifted 0.5 eV . Likewise, the maximum to minimum Li-O-D/O-C ratio varies 4% as opposed to a variation of 14% for Li-O/O-C.

B. Lithium and deuterium effects on carbon chemistry

The prominent C 1s peak for virgin ATJ graphite, shown in Fig. 4(b), is located at $283.7 \pm 0.6\text{ eV}$ and corresponds to graphitic bonds. A broad shoulder in XPS spectra indicates that other smaller peaks are convoluted within the larger peak. CO (285.3 eV) is found to contribute to the broad C 1s peak in Fig. 4(b).¹⁹ A small peak at $290.2 \pm 0.6\text{ eV}$ is also present and corresponds to carbonate bonds. For virgin graphite, integrating the XPS spectrum for these three regions indicates that graphitic bonds account for 77.7% of C 1s photoelectron spectrum, CO bonds account for 14.0% , and carbonate bonds account for 3.7% . The unaccounted percentage can be attributed to background signal. After lithium

deposition [see Fig. 4(b), 'Li: $2\text{ }\mu\text{m}$ '], the graphitic peak is suppressed, but few other changes are observed. Deuterium irradiation (fluence of $\sim 9 \times 10^{16}\text{ cm}^{-2}$) results in the development of a new peak at $291.2 \pm 0.6\text{ eV}$ [Fig. 4(b) labeled 'D2: 30']. Control experiments, shown in Fig. 4(e), show that irradiating virgin graphite without prior lithium conditioning does not result in the formation of this peak. Because the peak at 291.2 eV forms only when irradiating a lithiated sample, it is concluded that is a result of a Li-C-D interaction.

The Li 1s spectra are observed in Fig. 2(c). The photoelectron spectrum for lithium is less telling than oxygen and carbon simply because lithium has fewer electrons and therefore can produce fewer photoelectrons. Li 1s is positioned at $55.4 \pm 0.6\text{ eV}$ and deuterium irradiation is found to cause a shift to 56.2 eV . For pure lithium, the Li 1s peak is at $55.7\text{ eV} \pm 0.4\text{ eV}$.

C. Postmortem NSTX tile core samples

Four FY08 NSTX post-mortem tiles were removed and analyzed at Purdue University. Tiles were removed from the lower inner divertor, lower center stack, and upper passive plate near LiTER. NSTX tile A408-002 (Fig. 5) was removed from the lower divertor and its analysis is of interest due to the high lithium concentration that is deposited on the lower divertor. Samples were cored from the tile in a radial direction as represented in Fig. 5 (core sample number is appended to tile name; i.e., NSTX tile A408-002-5 corresponds to core sample 5).

XPS spectra of as-received tile core samples are not identical in each of the radial locations. Instead, XPS spectra taken from inboard locations (for example core samples 4 and 5) approach the private flux region (PFR) and exhibit more broad unordered peaks whereas samples cored from outboard locations and outside the PFR (core samples 1 and 2) have consistent, narrow peaks that are typical for XPS. Radial XPS comparisons show that the full width half max (FWHM) decreases for tile cores farther away from the PFR. The exact cause of these differences is unknown but is suspected, in part, to be an artifact of surface amorphization in addition to surface passivation and contamination upon air exposure.

The as received tile surface exhibits broad, unordered XPS peaks in O 1s, C 1s, and Li 1s energy ranges as shown in Fig. 6. The result of the previously outlined tile cleaning procedure commences with Ar sputtering followed by annealing. Results of sputtering are shown under the label 'Ar: 3h' and appear to morph the broad, unordered peaks and do not reveal spectra characteristic of lithiated graphite. Annealing the sample transforms the surface and yields peaks characteristic of XPS and in particular, lithiated graphite. Remarkably, the resulting spectrum has peak energies nearly identical to those observed in the laboratory experiments described above. For ease of comparison, post irradiation laboratory experimental spectra have been plotted inline with the spectra collected from NSTX tile A408-002-5. Peak positions vary by as much as 1.0 eV (for prominent peak in C 1s energy range), however in the O 1s energy range variations are within $\pm 0.3\text{ eV}$. In addition, the binding energy for each

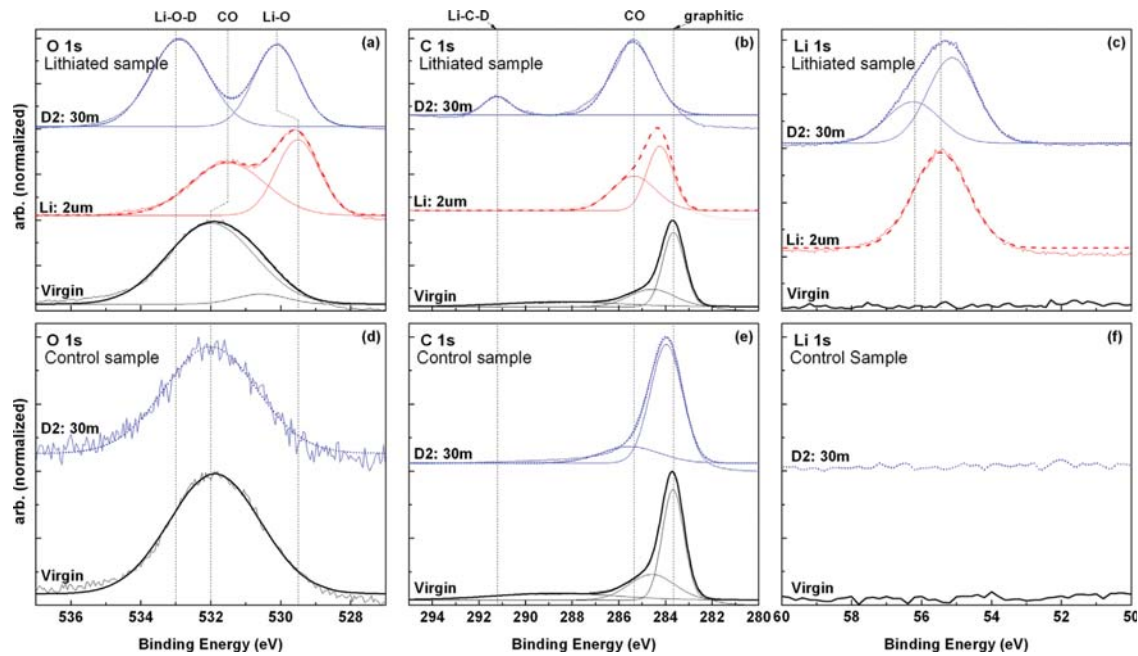


FIG. 4. (Color online) XPS spectra showing chemical interactions for two ATJ graphite substrates with lithium (top figures) and without lithium (bottom figures). Photoelectron spectra energy regions for (a) O 1s, (b) C 1s, and (c) Li 1s, for graphite sample with $2\ \mu\text{m}$ lithium deposited and exposed to a deuterium fluence of $9 \times 10^{16}\ \text{cm}^{-2}$. (d), (e), and (f) have no lithium deposition and a deuterium fluence of $6 \times 10^{16}\ \text{cm}^{-2}$. In the figure “D2” means irradiation with low-energy D_2^+ ions at 500 eV/amu and “30m” means thirty minutes irradiation.

functionality (Li-O, Li-C-D, etc.) is slightly lower for NSTX samples. Typically this would indicate a charging effect, however in this case it is unlikely as the shift is not uniform for all spectra. Instead, slight differences could be an artifact of prolonged air exposure and surface passivation, or possible disassociation of weak bonds. Regardless, the correlation between

NSTX tile samples and laboratory experiments is a clear indication of similar surface chemistry. These same functionalities are observed in other tiles located throughout NSTX, provided that tile locations have sufficient lithium coverage, and detail of their analysis will be the subject of future work. Because these peaks are observed in both laboratory experiments as well as post-mortem tiles, it can be inferred that lithium is responsible for deuterium retention, in the presence of oxygen and carbon. Furthermore, lithium will bind with oxygen and carbon whenever present, forming weak and strong interactions, and prevent the formation of simpler LiD bonds.

D. Implications of surface chemistry on deuterium recycling

The results discussed presently form a link showing that laboratory experiments can expound on, to some level, the behavior of fusion devices. Although the NSTX fusion environment invariably introduces many parameters that affect plasma material interactions, controlled laboratory experiments can represent the surface chemistry observed in post-mortem tiles. Since several parameters (graphite substrate, lithium conditioning, and deuterium irradiation) are found to be primary contributors to surface chemistry in experiments, these studies can therefore be extended to include computational modeling.

In NSTX, deuterium retention reduces recycling and improves plasma performance. As energetic deuterium is introduced to a lithiated graphite sample, Li-O-D and Li-C-D complexes form. Similar interactions are present for post-mortem samples. It can therefore be deduced that Li-O-D and Li-C-D interactions govern deuterium retention and therefore

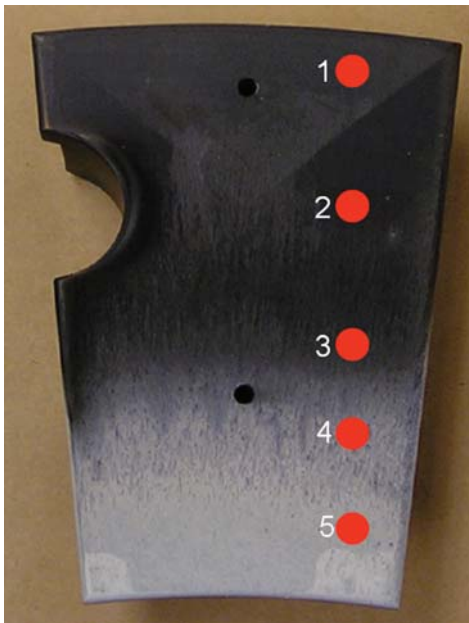


FIG. 5. (Color online) Photograph of the NSTX tile from which core samples were analyzed. Data represented in Fig. 6 were obtained from tile A408-002 at the locations approximated by point 5. Tile was removed from NSTX lower divertor.

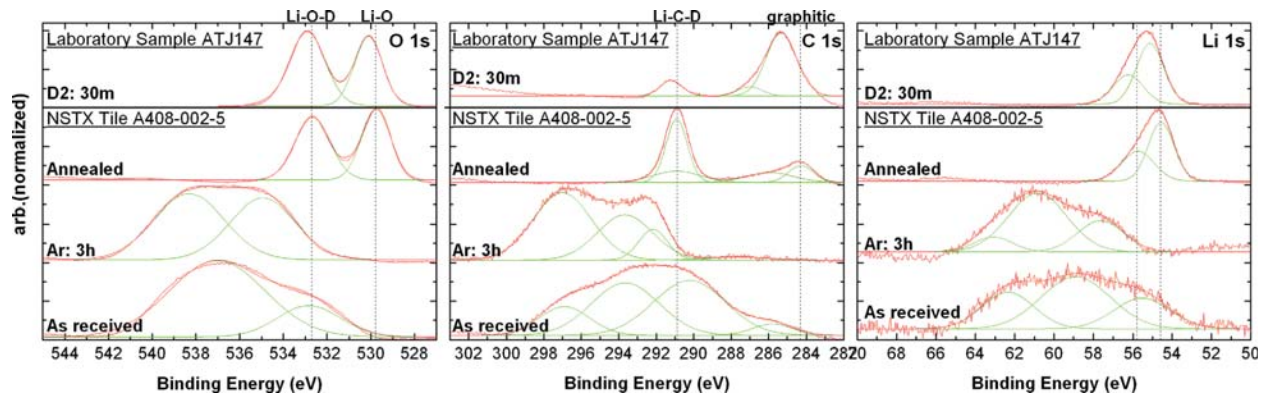


FIG. 6. (Color online) Ar sputtering and annealing procedure cleans and repairs NSTX tile sample A408-002-5 revealing surface chemistry similar to that of laboratory samples. Spectra labeled “Laboratory Sample ATJ147” are a subset of those shown in Fig. 4.

reduce recycling for graphite fusion devices that employ lithium wall conditioning.

IV. CONCLUSIONS

Surface characterization and analyses have been performed for ATJ graphite samples under controlled conditions as well as NSTX post-mortem tiles. X-ray photoelectron spectroscopy assists in identifying key chemical interactions that are associated with deuterium retention. Deuterium is found to induce Li-O-D and Li-C-D interactions/bonds with lithium in the presence of oxygen and carbon. Control experiments show that lithiated graphite has two prominent chemical interactions in the O 1s photoelectron energy range at 532.0 ± 0.6 eV and 529.5 ± 0.6 eV corresponding to O-C and Li-O. Deuterium irradiation results in the formation of an additional O 1s peak located at 532.9 ± 0.6 eV and is attributed to Li-O-D. Similarly, deuterium irradiation results in the formation of a peak in the C 1s photoelectron energy range at 291.2 ± 0.6 eV, indicative of Li-C-D interactions. Ar sputtering and annealing is found to clean and repair the passivated and amorphous surface found in postmortem tiles taken from the NSTX lower divertor private flux region. The resultant post-mortem XPS spectra correlate directly (± 0.3 eV) to the XPS peaks found in control laboratory experiments. XPS also indicates that lithium will always bind with oxygen and carbon, when present, and incoming deuterium will then interact with existing Li-O and Li-C structures.

ACKNOWLEDGMENTS

We would like to thank Purdue University Graduate School for providing student funding, L. Kollar and T. Morton for their contributions in running experiments and sample preparation, O. El-Atwani for his insights regarding data interpretation, and C. S. Skinner, H. W. Kugel, and A. L. Roquemore at the Princeton Plasma Physics Laboratory for their useful

discussion of post-mortem samples which they provided for this study. Work supported by US DOE Contract DE-FG02-08ER54990.

- ¹R. Maingi, T. Osborne, B. LeBlanc, R. Bell, J. Manickam, P. Snyder, J. Menard, D. Mansfield, H. Kugel, R. Kaita, S. Gerhardt, S. Sabbagh, and F. Kelly, *Phys. Rev. Lett.* **103**, 075001 (2009).
- ²M. G. Bell, H. Kugel, R. Kaita, L. E. Zakharov, H. Schneider, B. LeBlanc, D. Mansfield, R. Bell, R. Maingi, S. Ding, S. Kaye, S. Paul, S. Gerhardt, J. Canik, J. Hosea, G. Taylor, and T. Team, *Plasma Phys. Controlled Fusion* **51**, 124054 (2009).
- ³H. Kugel, M. G. Bell, J. Ahn, J. P. Allain, R. Bell, J. Boedo, C. Bush, D. Gates, T. Gray, and S. Kaye, *Phys. Plasmas* **15**, 056118 (2008).
- ⁴D. K. Mansfield, H. W. Kugel, R. Maingi, M. G. Bell, R. Bell, R. Kaita, J. Kallman, S. Kaye, B. LeBlanc, D. Mueller, S. Paul, R. Raman, L. Roquemore, S. Sabbagh, H. Schneider, C. H. Skinner, V. Soukhanovskii, J. Timberlake, J. Wilgen, and L. Zakharov, *J. Nucl. Mater.* **390-391**, 764 (2009).
- ⁵H. Kugel, M. G. Bell, R. Bell, C. Bush, D. Gates, T. Gray, R. Kaita, B. LeBlanc, R. Maingi, and R. Majeski, *J. Nucl. Mater.* **363**, 791 (2007).
- ⁶H. W. Kugel, M. G. Bell, L. Berzak, A. Brooks, R. Ellis, S. Gerhardt, H. Harjes, R. Kaita, J. Kallman, R. Maingi, R. Majeski, D. Mansfield, J. Menard, R. E. Nygren, V. A. Soukhanovskii, D. Stotler, P. Wakeland, and L. E. Zakharov, *Fusion Engineering and Design*, 1 (2009).
- ⁷B. Scrosati, *Electrochim. Acta* **45**, 2461 (2000).
- ⁸P. Chen, X. Wu, J. Lin, and K. L. Tan, *Science* **285**, 91 (1999).
- ⁹J.-M. Tarascon, *Nat. Chem.* **2**, 510 (2010).
- ¹⁰N. Itou, H. Toyoda, K. Morita, and H. Sugai, *J. Nucl. Mater.* **290**, 281 (2001).
- ¹¹H. Estrade-Szwarckopf and B. Rousseau, *Synth. Metals* **23**, 191 (1988).
- ¹²S. S. Harilal, J. P. Allain, A. Hassanein, M. R. Hendricks, and M. Nieto-Perez, *Appl. Surf. Sci.* **255**, 8539 (2009).
- ¹³M. Baldwin, R. Doerner, S. Luckhardt, and R. Conn, *Nucl. Fusion* **42**, 1318 (2002).
- ¹⁴C. N. Taylor, J. P. Allain, B. Heim, P. S. Krstic, C. H. Skinner, and H. W. Kugel, *J. Nucl. Mater.* **1** (2010).
- ¹⁵V. A. Soukhanovskii, (Preliminary assessment of) Recycling and particle fluxes in NSTX (2007).
- ¹⁶V. Soukhanovskii, R. Maingi, R. Bell, D. Gates, R. Kaita, H. Kugel, B. LeBlanc, R. Maqueda, J. Menard, and D. Mueller, *Arxiv* **0912**, 4281 (2009).
- ¹⁷NIST Standard Reference Database, available at www.nist.gov.
- ¹⁸M. Down and G. Whitlow, *J. Nucl. Mater.* **85**, 305 (1979).
- ¹⁹M. Phaner-Goutorbe, A. Sartre, and L. Porte, *Microsc. Microanal. Microstruct.* **5**, 283 (1994).